Modeling Ultrasonic Channels with Mobility for Gateway to In-Body Nanocommunication

Jorge Torres Gómez, Anke Kuestner, Lukas Stratmann, and Falko Dressler
School of Electrical Engineering and Computer Science, TU Berlin, Berlin, Germany

***Abstract*—Ultrasonic communication is one of the frequently discussed communication technologies for connecting in-body nanosensors with out-of-body gateway systems. Such communication has even been explored in various experimental setups. Yet, the impact of mobility remains primarily unexplored, which is critical for in-body applications. This paper aims to fill this gap by studying the impact of mobility on ultrasonic communication channels as the link between traveling nanosensors in the blood flow and external gateways fixed to the skin. We study both Doppler shift as well as signal gain both in an analytical model as well as in an extensive set of simulations. Our results indicate a significant impact of Doppler shift that needs to be compensated for real communication. We also show that the position of the nanosensors with respect to the gateway plays a very important role. Thus, we open the path for new research on protocol design for in-body to out-of-body communication using ultrasound.**

***Index Terms*—Nanocommunication, ultrasonic, in-body communication, doppler, mobility, nanosensor**

I. Introduction

Nano communication is a fundamental basis for future non-invasive medical solutions to cure diseases and to enhance the comfort of patients in general [1]. Among others, nanosensors are considered for patrolling the human circulatory system (HCS) and to coordinate with a gateway system outside of the body. To achieve this goal, a reference architecture has been proposed to *connect in-body networks to body area networks* [2], [3]. In-body networks are composed of nanosensors within the human body, e.g., flowing with the blood, and being connected to each other to measure health parameters or to deliver drugs to a specific target within the body [4], [5]. In contrast, body area networks interconnect all devices used on and around the body to measure and evaluate a patient's health parameters [6].

In Fig. 1, we outline a possible model for the connection of these two networks, based on a gateway located on the skin and nanosensors passing by with the blood circulation. The connection is particularly challenging as potential communication methods have to propagate through a very heterogeneous environment of the skin, tissue, blood vessels, and in some cases bones. Standard technologies enabling communication between nanosensors and the gateway focus on molecular communication (MC) [7]–[9], terahertz communication [10], [11], and ultrasound [12]–[15].

MC-based links can be a suitable solution for the interconnection of nanosensors within the HCS. For a communication link between nanosensors located inside blood vessels with a gateway that is not necessarily directly integrated into the

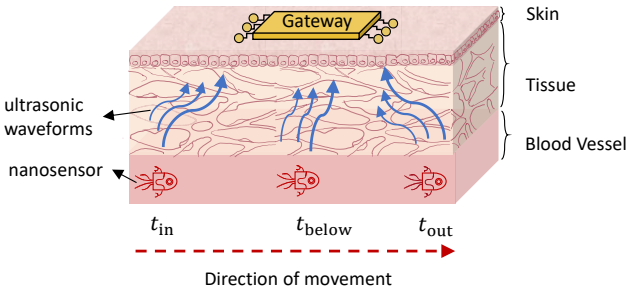

Fig. 1: Conceptual representation of the flowing nanosensor through a given blood vessel and its connection to the Gateway.

circulatory system, MC is a more challenging proposition [16]. This is because carrier particles would constantly have to permeate the blood vessel walls and, depending on the gateway location, even the skin.

Another considered communication technology are the terahertz waves, which are considered to be useful for short distances within the body. An alternative for communication between gateway and nanosensors is ultrasound communication enabling longer distances for connectivity within the body. Literature research contends theoretical schemes for ultrasound communications [17], and measurements indicate it presents a similar gain factor in human tissues as in water and is already used for various medical applications [12], [15], [18], [19]. As stated by Sciacca and Galluccio [12], therapies with ultrasounds are safe and do not damage the body.

In recent years, some experiments have been carried out to investigate the propagation of ultrasonic waveforms through in-body channels. This has been conceived with very small transducers and reported to evaluate propagation delay, excess delay, and the channel impulse response (CIR) [12]–[14]. However, these experiments considered only static distances among transmitter (gateway) and receiver (nanosensors). Mobility concerns, for scenarios like the one presented in Fig. 1, are not addressed in these reported studies. This matter becomes essential due to the distortions introduced by mobility as the nanosensors travel with the blood flow and the gateway is fixed to the skin. As described by the Doppler effect, the impact of mobility will inevitably degrade communication performance with time.

In this paper, we fill this gap and focus on the impact of mobility on ultrasonic communication. We propose an analytical model to address dynamic distances between transmitter

and receiver using ultrasonic in-body communication, caused by nanosensors moving constantly with the blood. Our model builds upon experimental data for signal gain and bit error rate (BER) as published in [13].

Our main contributions can be summarized as follows: 1) We developed an analytical model to address dynamic distances using ultrasonic in-body communication; 2) we performed an extensive set of Matlab simulations to evaluate the impact of movement; and 3) we discuss the impact of time-varying Doppler shift and signal gain on protocol design solutions.

Our study isolates the impact of the channel on communication performance. The resulting analysis provides the basis for designing synchronization mechanisms and protocols to establish the communication link.

II. Related Work

Recent years have brought up a lot of research and publications on the topic of ultrasound in-body communication channels. The communication channel can be described through various parameters, such as propagation speed and gain, which affect the received signal. Unfortunately, due to different experimental setups and different testbeds, the results are not always easily transferable. The sound *propagation speed* in human tissues is stated to be in the range of 1450–1540 m/s [12], [13], [18]; differently, it is assumed to be in the range of 330–3600 m/s in [15], considering not only tissue but for example gas and air bubbles in the lungs.

Other important parameters to look at in combination are the used *frequency* and the *distance* between sender and receiver since they have a strong impact on the gain of the received signal. In medical diagnostics, frequencies of 2–10 MHz play a role. For example, Santagati et al. [20] use frequencies up to 10 MHz and experience an acceptable gain based on a mathematical model. On the other hand, Bos et al. [13] consider 1.19 MHz to be the best frequency for distances of several centimeters based on a testbed.

To our knowledge, Sciacca and Galluccio [12] and Bos et al. [13] provide some of the best characterization of ultrasonic in-body communication channels. Through the usage of the *channel impulse response* they provide a general model for further research. The channel impulse response is of particular interest as it can be used to convolve an input signal to calculate the received signal after transmission [21]. Both groups have designed their own testbeds with gelatin phantoms, some with and some without animal bones, that mimic the human tissue and bones for the channel model. The consideration of animal bones is due to the fact that the phantoms should mimic the human body as realistically as possible.

Bos et al. [13] also considered two different scenarios, one mimicking implanted transducers and one mimicking transducers on the surface. For implanted transducers, they submersed the gelatin phantom into an anechoic water tank and for surface communication, the phantom was entirely surrounded by air. The testbeds used waveform generators to create the pulse to be transmitted for the transducer. While Sciacca and Galluccio [12] and Galluccio et al. [18] considered

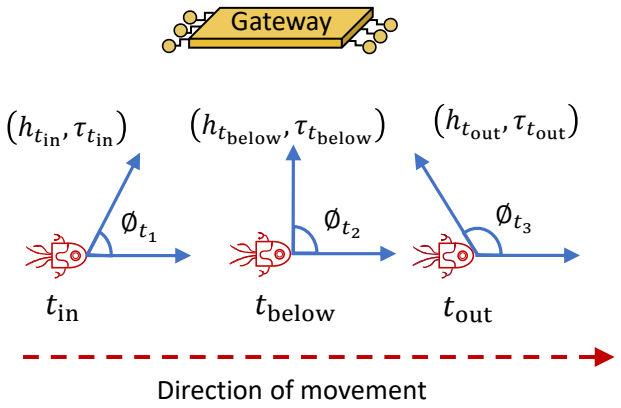

Fig. 2: System model. The flowing nanosensor navigates through a given blood vessel. Depicted are the relevant communication link properties at time steps t_{in} (nanosensor gets into communication range with the gateway), t_{below} (nanosensor is closest to the gateway), and t_{out} (nanosensor leaves the communication range).

5.5 cm, 10 cm, and 12 cm, Bos et al. [13] used 2 cm, 4 cm, and 8 cm distances between transmitter and receiver. At the receiver, the testbeds are using an oscilloscope to measure the amplitude of the received waveform and the delays of received echos.

The CIR is modeled with a low pass filter and coefficients are estimated through fitting techniques [12], [13]. The pure gelatin phantoms showed a similar channel behavior as a pure water channel, and multipath effects appear when experimenting with phantom and bones. Impact is reduced through more robust modulation techniques like spread spectrum systems [20].

III. Communication Model for LTV Ultrasound Channels

Without loss of generality, we assume that the nanosensor is traveling in a path trajectory from left to the right relative to the gateway device located on the skin, as depicted in Fig. 2. Taking into account the movement of the nanosensor, the communication performance between the two devices is modeled by a linear time-variant (LTV) channel and also includes the Doppler effect for the ultrasound communications. Due to the varying distance between the nanosensor and the gateway, the channel gain and delay will be time-dependent, as long as the distance between the nanosensor and the gateway device changes with time. The variables t_i highlight certain points in time during the movement process of a nanosensor. Timepoint t_{in} marks the time the nanosensor gets into the communication range of the gateway. Timepoint t_{below} marks the situation when the nanosensor is directly below the gateway and the angle of reception ϕ_{t_2} is, therefore, $\frac{\pi}{2}$. For every time instant t_i, there is a combination of (h_{t_i}, τ_{t_i}), where h_{t_i} describes the channel impulse response and τ_{t_i} describes the propagation delay for the current point in time.

To describe the impact of the LTV channel on the received signal $r(t)$ (ultrasonic waveform), we use the formula provided

in [22] as

$$r(t) = g_d s(t - \tau_d) e^{j2\pi\nu t}, \tag{1}$$

where $s(t)$, g_d, τ_d, and ν represent the transmitted signal, gain factor, delay, and Doppler frequency corresponding to the given distance between the nanosensor and the gateway, here denoted as d. The Doppler frequency can be obtained as

$$\nu = v \cos(\phi) \frac{f_c}{c_u}, \tag{2}$$

where v is the velocity of the nanosensor, c_u is the propagation speed of the ultrasonic waveform, f_c is the carrier frequency, and ϕ is the angle of arrival of the wave relative to the direction of motion of the nanosensor, as depicted in Fig. 2. For the in-body scenario, we consider typical velocities v of the nanosensor in the human circulatory system in the aorta ($v = 0.2\,\mathrm{m/s}$), arteries ($v = 0.1\,\mathrm{m/s}$), and veins ($v = 0.03\,\mathrm{m/s}$) [23].

According to Eq. (1), the impact of the LTV channel can be analyzed through the three different terms g_d, τ_d, and ν. The terms g_d and τ_d can be directly computed based on the distance between the nanosensor and the gateway, while the ν term is dependent on the dynamic of movement according to the path trajectory and the velocity (ϕ and v in Eq. (1)), as well as the communication parameters given by the center frequency f_c and the signal propagation speed c_u in Eq. (2).

We evaluate the three terms g_d, τ_d, and ν in Eq. (1), assuming that a nanosensor moves on a linear path trajectory from left to right, as depicted in Fig. 2. This results in a valid approximation for the traveling path of nanosensors, as they are driven through the laminar blood flow in the vessels [23]. To compute the gain and delay, we interpolate the results of the measurements given by [13],[1], where the CIR is provided for three specific distances 20, 40, and 80 mm between sender and receiver. Implicitly, through this CIR we are taking into account the impact of bones and the multipath effect already included in it. Firstly, we compute the gain factor for each distance as the root mean square (RMS) of the given CIR yielding

$$g_{d'} = \sqrt{\frac{1}{N} \sum_{k=1}^{N} h_{d'}^2[k]}, \tag{3}$$

where N is the length of the sequence and $h_{d'}[k]$ is the CIR for the given distance d', i.e., 20, 40, and 80 mm. For the delay, we compute the mean value (concerning time) plus the standard deviation of the CIR sequences as

$$\tau_{d'} = \overline{\tau}_{d'} + \frac{\tau_{\sigma,d'}}{2}, \tag{4}$$

where

$$\overline{\tau}_{d'} = \frac{1}{f_s} \frac{1}{N} \frac{\sum_{k=1}^{N} k \cdot h_{d'}^2[k]}{\sum_{k=1}^{N} h_{d'}^2[k]}, \tag{5}$$

and

$$\tau_{\sigma,d'} = \frac{1}{f_s} \sqrt{\frac{1}{N} \frac{\sum_{k=1}^{N} (k - f_s \overline{\tau}_{d'}) h_{d'}^2[k]}{\sum_{k=1}^{N} h_{d'}^2[k]}}, \tag{6}$$

[1]Published by Thomas Bos under the CC-BY-SA 4.0 license on GitHub https://github.com/BosThomas/USbodyComm

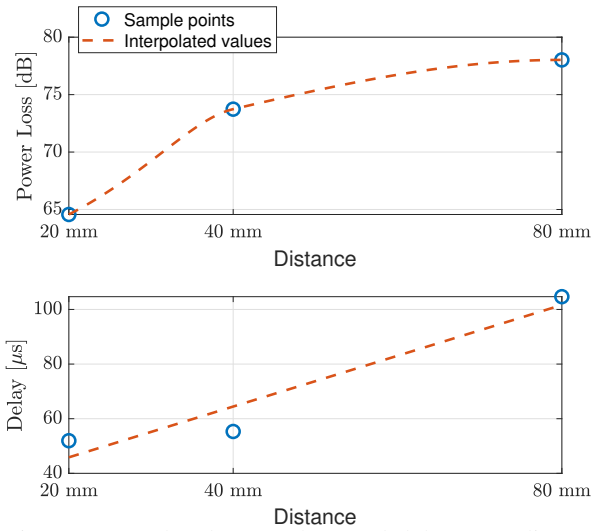

Fig. 3: Interpolated power loss and delay over distance.

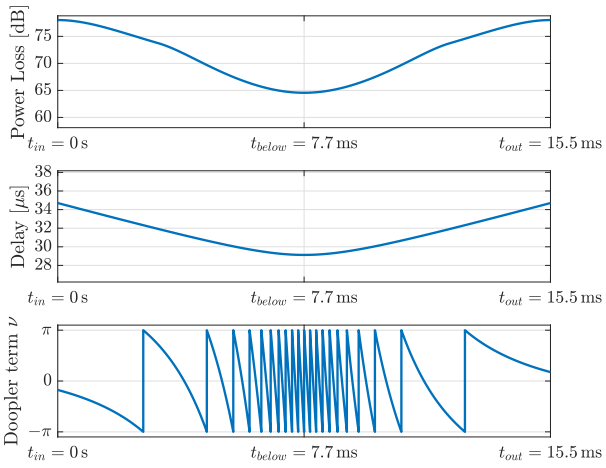

Fig. 4: Results on the perceived loss, delay, and the Doppler term on the travel path when the velocity of the nanosensor is $v = 0.2\,\mathrm{m/sec}$ and the carrier frequency is $f_c = 1\,\mathrm{MHz}$.

where f_s is the sampling rate of the system. These relations in Equations (5) and (6) evaluate the weighted arithmetic mean, where the weights are defined by the square of the CIR function to neglect its negative values.

Secondly, using the values provided in Equations (3) and (4) for the specific distances, interpolation is done to provide values for arbitrary distances between nanosensors and the gateway. To interpolate the gain, we use the "pchip" cubic interpolation method from Matlab as it provides a monotonic function for the arguments. To interpolate the delay, we fit a line to the measured delay due to its linear increase with the distance.

To evaluate the Doppler term, we directly compute the Eq. (2) according to the geometry in Fig. 2. Using trigonometric properties, we compute the angle between the nanosensor and the gateway for each different time-instant ϕ_t. As for the speed, we use the reported blood speeds in arteries ($v = 0.2\,\mathrm{m/s}$), capillaries, ($v = 0.1\,\mathrm{m/s}$), or veins ($v = 0.03\,\mathrm{m/s}$) [23]. For the communication parameters, we use the propagation speed

for the ultrasonic waveform as $c_u = 1480\,\mathrm{m/s}$, and a center frequency of $f_c = 1\,\mathrm{MHz}$.

To illustrate, Fig. 3 depicts the resulting interpolation for the power loss in decibels ($p_L = -20\log_{10}(g_d)$), and the delay in the communication range 20–80 mm. Using this curve, we evaluate the resulting gain and delay during the path trajectory of the nanosensor according to its specific distance to the gateway. The resulting evaluation is illustrated in Fig. 4 for the power loss, the delay, and Doppler term when assuming the traveling speed of 0.2 m/s in the aorta. As expected, the smallest power loss and delay are obtained when the nanosensor has the shortest distance to the gateway, i.e., for $t = t_{\text{below}} = 7.7\,\mathrm{ms}$, which corresponds to the position t_{below} in Fig. 2.

According to Fig. 4, the Doppler term (see Eq. (2)) will introduce a remarkable distortion on the received waveform. It will produce a phase shift in the range $[-\pi, \pi]$ rad along the traveling path. For instance, when considering the transmission of phase shift keying (PSK) waveforms, the impact of movement will severely rotate its constellation points, heavily degrading the communication performance. Analytically, this term introduces a rotation of the constellation coordinates with the angle

$$\Delta\varphi = 2\pi\nu t, \tag{7}$$

according to the exponential term in Eq. (1). The impact of movement on the communication performance is discussed in the next section.

IV. Simulation Results

To evaluate the impact of mobility in the communication performance, we simulated the channel model as given in Eq. (1) in Matlab. We assumed a propagation speed for the ultrasonic waveform as $c_u = 1480\,\mathrm{m/s}$. To illustrate, we performed simulations in which we transmitted a binary phase shift keying (BPSK) waveform, as indicated in [13], with a transmission rate of 10 kbit/s and of amplitude $A = 1$. Furthermore, we assumed the root mean square (AWGN) model (as given in [13]) to evaluate the impact of noise.

The effects on the recovered constellation points at a center frequency of 1 MHz and a nanosensor velocity of 0.03 m/s in the veins can be observed in Fig. 5, with signal to noise ratio (SNR) equal to $15\,\mathrm{dB}$. The transmission starts while the nanosensor is at the position provided by $t_{\text{in}} = 0\,\mathrm{ms}$ corresponding to the largest distance between both as $80\,\mathrm{mm}$, as depicted in Fig. 1. Although constant noise level produces spreading, the impact of mobility is clearly visible in the rotation of the constellation points, represented by the angle $\Delta\varphi$ (cf. Eq. (7)). The emitted coordinates $(-A, 0)$ and $(A, 0)$ are rotated over time to $(0, -A)$ and $(0, A)$, respectively. This is produced by the dominating Doppler factor ν as depicted in Fig. 4 (cf. Eq. (2)). The produced rotation of the constellation produces a severe degradation of the BER when decoding the received BPSK waveform.

To further investigate the effects produced through motion, we looked at the BER and the $\frac{E_b}{N_o}$ for varying parameters such as frequency, the velocity of the nanosensor, and position of

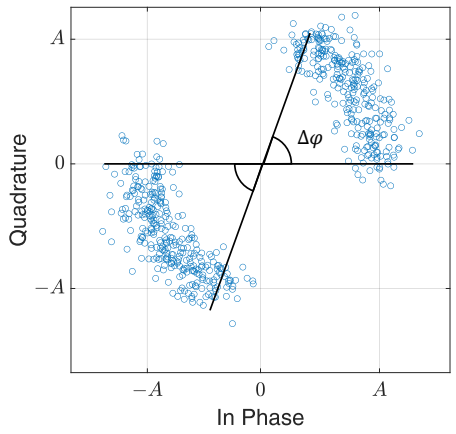

Fig. 5: Recovered constellation points for a nanosensor traveling speed of $0.03\,\mathrm{m/sec}$, SNR $= 15\,\mathrm{dB}$, and a center frequency $f_c = 1\,\mathrm{MHz}$.

the nanosensor to the start of transmission, where we also assumed a noise spectral density of $N_o = -117\,\mathrm{dB/Hz}$ [13]. Fig. 6 illustrates the results when the communication starts at $t_{\text{in}} = 0\,\mathrm{ms}$, corresponding to the largest distance between the nanosensor and the gateway at 80 mm, and till the BER is degraded to 0.5 units. The evolution of the BER curve over time, as shown in Fig. 6 a), is obtained when evaluating it according to $\text{BER} = \frac{1}{2}\,\text{ercf}\left(\sqrt{\frac{E_b}{N_o}}\right)$ [21], where $E_b = \frac{A_r^2}{2}\cos^2(\varphi)T_b$ is the energy of the received bit, A_r is the amplitude of the received waveform, φ is the angle of the received constellation point, T_b is the duration of one bit, and N_o is the noise spectral density. The evolution of the $\frac{E_b}{N_o}$, as illustrated in Fig. 6, is obtained after directly evaluating $E_b = \frac{A_r^2}{2}\cos^2(\varphi)T_b$ in the ratio $\frac{E_b}{N_o}$ for each different location of the nanosensor.

According to these expressions and the obtained results, the perceived degradation is mainly given by the impact of the Doppler factor on the constellation points, i.e., the energy of the decoded bit is reduced by the value of $\cos(\varphi)$ when φ approaches $\frac{\pi}{2}$. The energy of the received signal will be not only given by the channel gain (resulting A_r) but also by the Doppler effect (resulting in a rotated constellation). Due to this effect, the initial 15 dB becomes –40 dB in less than 5 ms for the different frequencies of transmissions (cf. Fig. 6).

To evaluate the impact of the nanosensor speed through different vessel segments, Fig. 7 depicts the obtained BER curves in the aorta ($v = 0.2\,\mathrm{m/s}$), arteries ($v = 0.1\,\mathrm{m/s}$), and veins ($v = 0.03\,\mathrm{m/s}$) [23]. As expected, the less degraded curve is derived for the lowest speed, i.e., in the veins. This is the best point in time to establish communication between nanosensors and external devices to reduce the impact of the Doppler effect.

However, starting the communication at t_{in} also implies the less favorable angle ϕ concerning the Doppler frequency in Eq. (2). To reduce the impact of Doppler effects, the best communication link is in the range around the time instant t_{below}, where ϕ is close to $\frac{\pi}{2}$ yielding $\nu \to 0$ and therefore

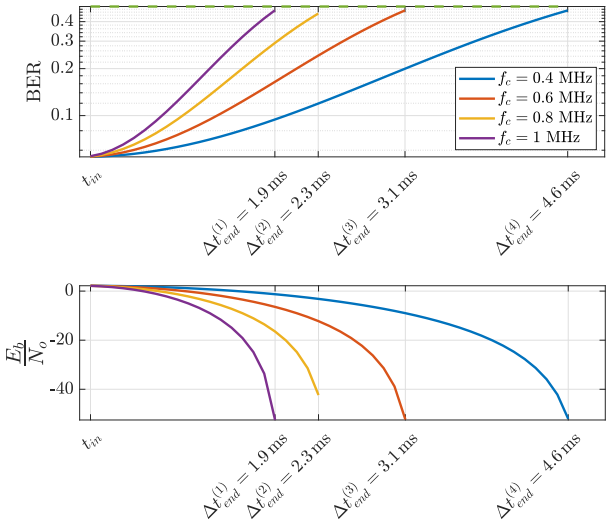

Fig. 6: Achievable BER versus time when the velocity of the nanosensor is $0.2\,\mathrm{m/sec}$ (aorta segment). The communication between the nanosensor and the gateway starts at $t_{\text{in}} = 0\,\mathrm{ms}$ corresponding to the largest distance between both as $80\,\mathrm{mm}$, as depicted in Fig. 1.

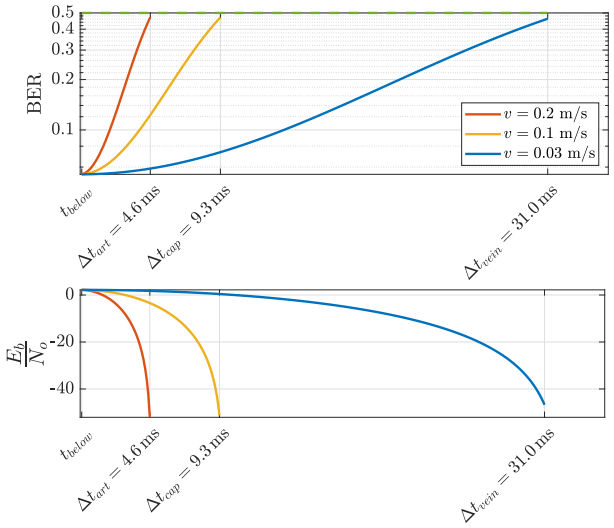

Fig. 7: Achievable BER versus time when the center frequency of the emitted BPSK waveform is $0.4\,\mathrm{MHz}$. The communication between the nanosensor and the gateway starts at $t_{\text{in}} = 0\,\mathrm{ms}$ corresponding to the largest distance between both as $80\,\mathrm{mm}$, as depicted in Fig. 1.

$\Delta\varphi \to 0$. Correspondingly, the impact on the constellation rotation is less as long as the resulting $\Delta\varphi$ is close to zero.

Figures 8 and 9 depict the BER when the communication starts at $t_{\text{below}} = 50\,\mathrm{ms}$ corresponding to the shortest distance between both at $20\,\mathrm{mm}$, as depicted in Fig. 1, and till the BER is degraded to 0.5 units. As can be seen in these figures, the possible communication time increases at least three times for the veins compared to their counterparts in Figures 6 and 7. That is, when considering the BER $= 0.5$, the time interval for transmissions in the veins is around 50.9 ms when starting

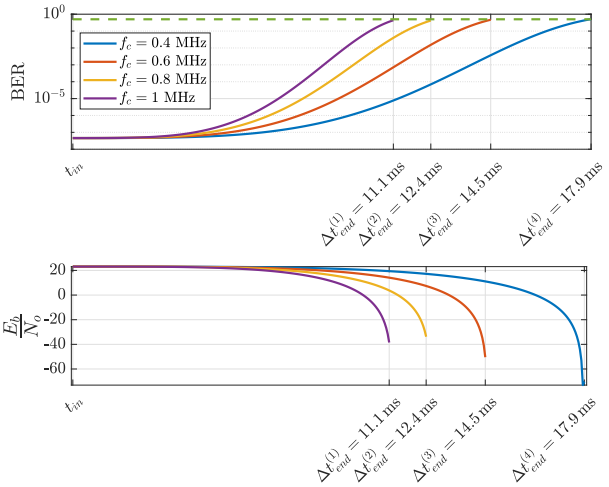

Fig. 8: Achievable BER versus time when the velocity of the nanosensor is $0.2\,\mathrm{m/sec}$ (aorta vessel segment). The communication between the nanosensor and the gateway starts at $t_{\text{below}} = 50\,\mathrm{ms}$ corresponding to the shortest distance between both as $20\,\mathrm{mm}$, as depicted in Fig. 1.

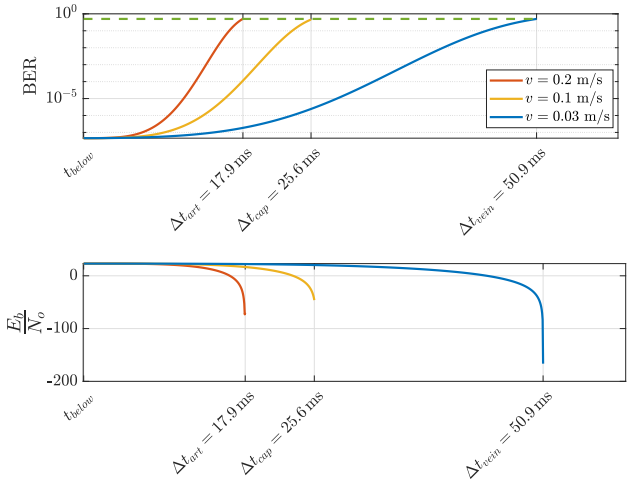

Fig. 9: Achievable BER versus time when the center frequency of the emitted BPSK waveform is $0.4\,\mathrm{MHz}$. The communication between the nanosensor and the gateway starts at $t_{\text{below}} = 50\,\mathrm{ms}$ corresponding to the shortest distance between both as $20\,\mathrm{mm}$, as depicted in Fig. 1.

transmission at t_{below} (cf. Fig. 9), while in the case of starting transmissions at t_{in} the time interval is reduced to 31.0 ms.

The resulting lower BER in Figures 8 and 9 is a consequence of the improved $\frac{E_b}{N_o}$ due to the closest distance to the gateway and the non-rotation of the constellation points at t_{below}. The power loss experienced at t_{below} results in 18 dB less that at t_{in} (cf. Fig. 4). Consequently, $\frac{E_b}{N_o}$ is increased in the same amount in comparison to Figures 6 and 7. Furthermore, the data rate can be increased as a result of the very small BER around t_{below}. This means that the communication performance strongly depends on the path of the nanosensor.

We see this work as a starting point for smart communication protocols that synchronize communication with the location

of the nanosensors with respect to the gateway. According to these results, whenever the communication starts below the gateway (t_{below} in Fig. 1) the communication time is increased. Consequently, this will introduce less overhead, as preambles get less, when conceiving synchronization mechanisms between the nanosensors and the gateway.

V. Conclusion

The connection of in-body nanosensors with out-of-body gateway systems plays a crucial role in future health care approaches. Among others, ultrasound is suggested for the communication link between these nodes. However, current models and also experiments only focus on stationary cases; which we extended using analytical and simulation models for mobile scenarios, where the Doppler shift plays an important role. The use of analytical models for LTV channels allows analyzing the communication performance. Due to the mobility of nanosensors, when traveling through the human circulatory system, the Doppler effect deteriorates significantly the perceived BER in their communication link with external devices. Our results indicate significant frequency shifts, which result in phase shifts and bit errors. We see this study as a basis for future protocol concepts that compensate for the effects by synchronizing the communication with the location of the nanosensors with respect to the gateway system.

Future work includes higher order modulation like MPSK, and studies of non-constant velocities of the nanosensors and the impact on the communication channel. Since we assume that the nanosensors are transported by the bloodstream, it must be addressed how the different velocities of the blood can be modeled. This is also related to changing gain factors due to different tissue materials (blood, bones, other tissues). We also plan to integrate the models for ultrasound in-body channels into our ns3-based simulation framework C-BVS [16], [24] to study the communications in a larger scale.

Acknowledgment

Reported research was supported in part by the project MAMOKO funded by the German Federal Ministry of Education and Research (BMBF) under grant numbers 16KIS0917 and by the project NaBoCom funded by the German Research Foundation (DFG) under grant number DR 639/21-1.

References

[1] L. Felicetti, M. Femminella, G. Reali, and P. Liò, "A Molecular Communication System in Blood Vessels for Tumor Detection," in *1st ACM International Conference on Nanoscale Computing and Communication (NANOCOM 2014)*, Atlanta, GA: ACM, May 2014.

[2] F. Dressler and S. Fischer, "Connecting In-Body Nano Communication with Body Area Networks: Challenges and Opportunities of the Internet of Nano Things," *Elsevier Nano Communication Networks*, vol. 6, pp. 29–38, Jun. 2015.

[3] I. F. Akyildiz and J. M. Jornet, "The Internet of Nano-Things," *IEEE Wireless Communications*, vol. 17, no. 6, pp. 58–63, Dec. 2010.

[4] A. V. Singh, M. H. D. Ansari, P. Laux, and A. Luch, "Micro-nanorobots: important considerations when developing novel drug delivery platforms," *Expert Opinion on Drug Delivery*, vol. 16, no. 11, pp. 1259–1275, Oct. 2019.

[5] M. Stelzner, F. Dressler, and S. Fischer, "Function Centric Nano-Networking: Addressing Nano Machines in a Medical Application Scenario," *Elsevier Nano Communication Networks*, vol. 14, pp. 29–39, Dec. 2017.

[6] M. Chen, S. Gonzalez, A. Vasilakos, H. Cao, and V. C. Leung, "Body Area Networks: A Survey," *ACM/Springer Mobile Networks and Applications (MONET)*, vol. 16, no. 2, pp. 171–193, Apr. 2011.

[7] B. Atakan, O. B. Akan, and S. Balasubramaniam, "Body Area NanoNetworks with Molecular Communications in Nanomedicine," *IEEE Communications Magazine (COMMAG)*, vol. 50, no. 1, pp. 28–34, Jan. 2012.

[8] N. Farsad, H. B. Yilmaz, A. W. Eckford, C.-B. Chae, and W. Guo, "A Comprehensive Survey of Recent Advancements in Molecular Communication," *IEEE Communications Surveys & Tutorials*, vol. 18, no. 3, pp. 1887–1919, 2016.

[9] J. Torres Gómez, K. Pitke, L. Stratmann, and F. Dressler, "Age of Information in Molecular Communication Channels," *Elsevier Digital Signal Processing (DSP), Special Issue on Molecular Communication*, vol. 124, p. 103 108, May 2022.

[10] J. M. Jornet and I. F. Akyildiz, "Channel Modeling and Capacity Analysis for Electromagnetic Wireless Nanonetworks in the Terahertz Band," *IEEE Transactions on Wireless Communications (TWC)*, vol. 10, no. 10, pp. 3211–3221, Oct. 2011.

[11] P. Wang, J. M. Jornet, M. A. Malik, N. Akkari, and I. F. Akyildiz, "Energy and spectrum-aware MAC protocol for perpetual wireless nanosensor networks in the Terahertz Band," *Elsevier Ad Hoc Networks*, vol. 11, no. 8, pp. 2541–2555, Nov. 2013.

[12] E. C. Sciacca and L. Galluccio, "Impulse response analysis of an ultrasonic human body channel," *Elsevier Computer Networks (COMNET)*, vol. 171, p. 107 149, Apr. 2020.

[13] T. Bos, W. Jiang, J. D'hooge, M. Verhelst, and W. Dehaene, "Enabling Ultrasound In-Body Communication: FIR Channel Models and QAM Experiments," *IEEE Transactions on Biomedical Circuits and Systems*, pp. 135–144, Feb. 2019.

[14] G. E. Santagati, N. Dave, and T. Melodia, "Design and Performance Evaluation of an Implantable Ultrasonic Networking Platform for the Internet of Medical Things," *IEEE/ACM Transactions on Networking (TON)*, vol. 28, no. 1, pp. 29–42, 2020.

[15] B. Jaafar, J. A. Neasham, and P. Degenaar, "What is Ultrasound Can and Cannot Do in The Communication of Biomedical Implanted Medical Devices," *IEEE Reviews in Biomedical Engineering*, vol. 14, May 2021.

[16] A. Kuestner, L. Stratmann, R. Wendt, S. Fischer, and F. Dressler, "A Simulation Framework for Connecting In-Body Nano Communication with Out-of-Body Devices," in *7th ACM International Conference on Nanoscale Computing and Communication (NANOCOM 2020)*, Virtual Conference: ACM, Sep. 2020.

[17] Q. Wang, Q. Guan, J. Cheng, and B. Ma, "Ultrasonic Indexed Modulation and Multiple Access for Intra-Body Networks," *IEEE Transactions on Communications*, vol. 69, no. 5, pp. 108–120, 2021.

[18] L. Galluccio, T. Melodia, S. Palazzo, and G. E. Santagati, "Challenges and Implications of Using Ultrasonic Communications in Intra-body Area Networks," in *9th IEEE/IFIP Conference on Wireless On demand Network Systems and Services (WONS 2012)*, Courmayeur, Italy: IEEE, Jan. 2012, pp. 182–189.

[19] T. Hogg and R. A. Freitas Jr., "Acoustic communication for medical nanorobots," *Elsevier Nano Communication Networks*, vol. 3, no. 2, pp. 83–102, Jun. 2012.

[20] G. E. Santagati, T. Melodia, L. Galluccio, and S. Palazzo, "Medium Access Control and Rate Adaptation for Ultrasonic Intrabody Sensor Networks," *IEEE/ACM Transactions on Networking (TON)*, vol. 23, no. 4, pp. 1121–1134, Aug. 2015.

[21] A. B. Carlson, P. B. Crilly, and J. C. Rutledge, *Communication Systems: An Introduction to Signals and Noise in Electrical Communication*, 4th ed. New York City, NY: McGraw-Hill, 2002.

[22] G. Matz and F. Hlawatsch, "Fundamentals of Time-Varying Communication Channels," in *Wireless Communications Over Rapidly Time-Varying Channels*, F. Hlawatsch and G. Matz, Eds., Elsevier, 2011, pp. 1–63.

[23] A. C. Guyton and M. E. Hall, *Guyton and Hall Textbook of Medical Physiology*, 14th ed. Elsevier, 2015.

[24] A. Kuestner, K. Pitke, J. Torres Gómez, R. Wendt, S. Fischer, and F. Dressler, "Age of Information in In-Body Nano Communication Networks," in *8th ACM International Conference on Nanoscale Computing and Communication (NANOCOM 2021)*, Virtual Conference: ACM, Sep. 2021.